World Journal of Gastroenterology

Submit a Manuscript: http://www.wjgnet.com/esps/
Help Desk: http://www.wjgnet.com/esps/helpdesk.aspx
DOI: 10.3748/wjg.v21.i34.10008

World J Gastroenterol 2015 September 14; 21(34): 10008-10017
ISSN 1007-9327 (print) ISSN 2219-2840 (online)

ORIGINAL ARTICLE

Observational Study

Computed tomography and magnetic resonance imaging features of lipid-rich neuroendocrine tumors of the pancreas

Yoshihiko Fukukura, Toshikazu Shindo, Michiyo Higashi, Koji Takumi, Tomokazu Umanodan, Tomohide Yoneyama, Takashi Yoshiura

Yoshihiko Fukukura, Toshikazu Shindo, Koji Takumi, Tomokazu Umanodan, Tomohide Yoneyama, Takashi Yoshiura, Department of Radiology, Kagoshima University Graduate School of Medical and Dental Sciences, Kagoshima City 890-8544, Japan

Michiyo Higashi, Department of Human Pathology, Kagoshima University Graduate School of Medical and Dental Sciences, Kagoshima City 890-8544, Japan

Author contributions: Fukukura Y designed the research and wrote the paper; Shindo T, Takumi K, Umanodan T, Yoneyama T and Higashi M analyzed and interpreted the data; Yoshiura T revised the article critically for important intellectual content; all authors participated in drafting or revising the article, and approved the submitted manuscript.

Institutional review board statement: This study was institutionally approved by Kagoshima University Graduate School of Medical and Dental Sciences.

Informed consent statement: The institutional review board did not require informed consent for a retrospective study using medical records or imaging examinations.

Conflict-of-interest statement: There are no competing interests to disclose in relation to this study.

Data sharing statement: No additional data are available.

Correspondence to: Yoshihiko Fukukura, MD, PhD, Department of Radiology, Kagoshima University Graduate School of Medical and Dental Sciences, 8-35-1 Sakuragaoka, Kagoshima City 890-8544, Japan. fukukura@m.kufm.kagoshima-u.ac.jp
Telephone: +81-99-2755417
Fax: +81-99-2651106

Received: March 19, 2015
Peer-review started: March 25, 2015
First decision: April 13, 2015
Revised: April 26, 2015
Accepted: July 15, 2015
Article in press: July 15, 2015
Published online: September 14, 2015

Abstract

AIM: To clarify the computed tomography (CT) and magnetic resonance imaging (MRI) characteristics of lipid-rich pancreatic neuroendocrine tumors (PanNETs).

METHODS: Enhanced CT and MRI performed before pancreatectomy in 29 patients with 34 histologically-confirmed PanNETs was retrospectively reviewed. Tumor attenuation on CT and signal intensities on conventional (T1- and T2-weighted) and chemical shift MRI were qualitatively analyzed and compared alongside adipose differentiation-related protein (ADRP) immunostaining (ADRP-positive: lipid-rich; ADRP-negative: non-lipid-rich) results using Fisher's exact test or the Mann-Whitney *U* test. Signal intensity index on chemical shift MRI was quantitatively assessed.

RESULTS: There were 15 lipid-rich PanNETs (44.1%) in 12 patients (41.4%). Tumor attenuation during the early, portal venous, and delayed phases of enhanced CT (P = 0.888, 0.443, and 0.359, respectively) and signal intensities on conventional MRI (P = 0.698 and 0.798, respectively) were not significantly different

between lipid-rich and non-lipid-rich PanNETs. Four of the 15 lipid-rich PanNETs exhibited high signal intensity on subtraction chemical shift MRI, and the association of high signal intensity on subtraction imaging with lipid-rich PanNETs was significant (4 of 15 lipid-rich PanNETs, 26.73%, *vs* 0 of 19 non-lipid-rich PanNETs, 0%, $P = 0.029$). Lipid-rich PanNETs showed a significantly higher signal intensity index than non-lipid-rich PanNETs (0.6% ± 14.1% *vs* -10.4% ± 14.4%, $P = 0.004$). Eight of 15 lipid-rich PanNETs, *vs* 0 of 19 non-lipid-rich PanNETs, had positive signal intensity index values in concordance with lipid contents.

CONCLUSION: CT contrast enhancement and conventional MR signal intensities are similar in lipid-rich and non-lipid-rich PanNETs. Chemical shift MRI can demonstrate cytoplasmic lipids in PanNETs.

Key words: Neoplasms; Chemical shift magnetic resonance imaging; Pancreas; Computed tomography; Neuroendocrine tumors

Core tip: Little is known about lipid-rich pancreatic neuroendocrine tumors (PanNETs). In the current study, we clarify computed tomography (CT) and magnetic resonance imaging (MRI) characteristics of lipid-rich PanNETs. Adipose differentiation-related protein antibody positive lipid-rich cells were observed in 15 of 34 tumors (44.1%). Lipid-rich PanNETs had a similar appearance to usual PanNETs on enhanced CT. On chemical shift MRI, positive signal intensity index values in concordance with lipid contents were observed in eight of 34 tumors (23.5%). Lipid-rich PanNETs should be included in differential diagnosis whenever chemical shift MRI demonstrates lipid components within hypervascular pancreatic tumors.

Fukukura Y, Shindo T, Higashi M, Takumi K, Umanodan T, Yoneyama T, Yoshiura T. Computed tomography and magnetic resonance imaging features of lipid-rich neuroendocrine tumors of the pancreas. *World J Gastroenterol* 2015; 21(34): 10008-10017 Available from: URL: http://www.wjgnet.com/1007-9327/full/v21/i34/10008.htm DOI: http://dx.doi.org/10.3748/wjg.v21.i34.10008

INTRODUCTION

Pancreatic neuroendocrine tumors (PanNETs) originate from pluripotent ductal stem cells and show endocrine differentiation[1]. The estimated prevalence of PanNET is 2.2 per million persons per year[2]. Microscopically, these tumors are usually composed of small, relatively uniform cuboidal cells with a finely granular eosinophilic or amphophilic cytoplasm that may be arranged into trabeculae, festoons, or solid nests[3]. Lipid-rich tumors are a distinct histological variant of PanNET that have cells characterized by an abundant, clear, and vacuolated cytoplasm; this substantial deviation from the usual appearance can pose diagnostic problems at biopsy[3-7]. However, the clinicopathological characteristics of lipid-rich PanNET and its difference from the usual PanNET remain unclear.

Diagnostic imaging is important for differentiating PanNETs from other pancreatic lesions in order to guide therapeutic strategy. Enhanced computed tomography (CT) and magnetic resonance imaging (MRI) are widely accepted techniques for detecting and characterizing pancreatic lesions. Due to their rich blood capillary network, typical PanNETs hyperattenuate relative to the surrounding pancreatic parenchyma during the early or portal venous phase of contrast enhanced CT[8,9]. PanNET appears as a relatively hypointense mass on T1-weighted images and most PanNETs demonstrate much higher signal intensities than normal pancreas on T2-weighted images[9,10]. However, the CT and MRI features of lipid-rich PanNETs have not yet been described.

Chemical shift MRI has been clinically applied in the field of body imaging to detect small amounts of lipids based on the inherent difference in the resonant frequencies of water and fat protons[11,12]. Radiologic detection of lipid components within pancreatic lesions has been evaluated for a variety of pancreatic lesions, and this information has been reported to enable radiologists to differentiate lipid-containing pancreatic lesions from PanNETs[13-18]. However, there have been no reports regarding the utility of chemical shift MRI for the detection of intracytoplasmic lipids associated with lipid-rich PanNETs.

Therefore, the purpose of the current study was to clarify the CT and MRI characteristics of lipid-rich PanNETs.

MATERIALS AND METHODS

Study population

Approval from the institutional ethics review board of the Kagoshima University Graduate School of Medical and Dental Sciences (Kagoshima City, Japan) was obtained and informed consent was waived for this retrospective study. *Via* review of clinical charts and records from the Department of Human Pathology, a total of 51 patients with pathologically-confirmed PanNET following surgical resection between April 2001 and June 2013 were retrospectively identified. Among these patients, 30 underwent three-phase enhanced CT (including early, portal venous, and delayed phases) and chemical shift MRI before pancreatectomy. The mean interval between imaging and surgical resection was 36.4 d (range, 4-77 d). Twenty-seven patients had unifocal PanNETs. One patient with a PanNET measuring 7 mm in diameter that was not visualized on CT and MRI was excluded. In three patients with

multifocal tumors, tumors with a maximum diameter < 10 mm were excluded because they were too small to evaluate on CT or MRI. One of the patients with multifocal PanNETs had one tumor ⩾ 10 mm, while another two patients had three and four, respectively. Thus, the final study population was comprised of 29 patients (13 men, 16 women; mean age, 55.8 years; range, 18-76 years) with 34 PanNETs. All clinical data, morphologic imaging findings (three-phase enhanced CT and MRI), and pathologic records for all patients were collected by the study coordinator, who had 20 years of abdominal radiology experience. Two patients had multiple endocrine neoplasia type 1 (MEN-1) and one had von Hippel-Lindau disease. Fourteen patients had hyperfunctioning endocrine tumors (9 insulinomas, 2 gastrinomas, and 3 glucagonomas). Tumor sizes ranged from 11 to 119 mm (mean, 24.1 mm), and tumors were located in the head (*n* = 14), body (*n* = 10), or tail (*n* = 10) of the pancreas.

Histopathological analysis

Following surgical resection, the final diagnosis was confirmed by a pathologist with 20 years of experience in pathological evaluation. The pathologist evaluated pathological tumor grade on the basis of the World Health Organization (WHO) classification[19], and reported the percentages of clear cells (based on findings of an abundant, clear, and vacuolated cytoplasm after hematoxylin-eosin staining of surgical specimens) and lipid-rich cells in each tumor. Lipid-rich cells were identified by immunohistochemical staining for adipose differentiation-related protein (ADRP) antibody (monoclonal antibody ADFP/AP125, 1:100, mouse IgG, NOVUS Biologicals, Littleton, CO, United States). All sections were stained on a Benchmark XT automated slide stainer using a diaminobenzidine detection kit (Ventana Medical Systems, Tucson, AZ, United States).

CT imaging technique

CT was performed on single- or multi-detector (16 or 64) row CT scanners using any of three CT units (Xvigor or Aquilion; Toshiba Medical Systems, Tokyo, Japan). All scans began at the top of the liver and continued through to the end of the pancreas. Imaging parameters for all phases of single-detector row CT (*n* = 7) included: 3 mm collimation, 3 mm reconstruction intervals using 120 kVp and 250 mA, and a 1:1 table pitch. Imaging parameters for multi-detector row CT (*n* = 22) were as follows: tube voltage, 120 kVp; gantry rotation speed, 0.5 s; maximum allowable tube current, 440 mA; detector row configuration, 16 mm × 1 mm for 16-detector row CT (*n* = 6) or 64 mm × 0.5 mm for 64-detector row CT (*n* = 16); and table increment, 15 mm/rotation for 16-detector row CT or 26.5 mm/rotation for 64-detector row CT. Early and portal venous phase scans were obtained at 30 and 70 s after starting infusion of contrast medium with single-detector row CT. With multi-detector row CT, they were obtained at delays of 23 s and 50 s after the bolus-tracking program detected the threshold aortic enhancement of 50 Hounsfield units. Scan delay for the delayed phase was fixed at 180 s after contrast injection. In each contrast-enhanced CT examination, a 100 mL or 2 mL/kg body weight of non-ionic contrast material with an iodine concentration of 300 mg I/mL (Iopamiron, Bayer Schering Pharma, Osaka, Japan or Omnipaque, Daiichi Sankyo, Tokyo, Japan) was intravenously injected at a fixed duration of 30 s.

MRI technique

MR images were obtained with 1.5-T [Magnetom Vision, Siemens, Erlangen, Germany (*n* = 9) or Excelart Vantage, Toshiba Medical Systems, Otawara, Japan (*n* = 6)] or 3.0-T system [Magnetom Trio, Siemens AG, Erlangen, Germany (*n* = 10) or Ingenia, Philips, Best, the Netherlands (*n* = 4)]. Chemical shift MRI was performed with a breath-hold 2D sequence with the 1.5-T (*n* = 15) and one of the 3.0-T MR systems (*n* = 4), and with a 3D dual gradient-echo sequence with the other 3.0-T MR system (*n* = 10). The MRI protocol and pulse sequence parameters are reported in Table 1. The subtraction chemical shift MR images were obtained by subtracting the series of out-of-phase images from the series of in-phase images using commercially available software integrated in the MR system.

Fat-suppressed T2-weighted images were obtained with a breath-hold single-shot turbo spin-echo (*n* = 9) or a respiratory-triggered multi-shot turbo spin-echo sequence (*n* = 20).

Qualitative image analysis

Two board-certified radiologists with 13 and 15 years of experience in abdominal radiology, respectively, independently assessed tumor-node-metastasis (TNM) stage according to the European Neuroendocrine Tumor Society of PanNETs [20] on CT and MRI. Tumor involvement of the celiac axis or superior mesenteric artery was considered if the artery showed that more than a half of its circumference was contiguous with the tumor[21]. The presence of lymph nodes with a short-axis diameter > 10 mm was regarded as lymph node metastases[22]. Tumor margins (sharp or irregular) and interruption of the main pancreatic duct with upstream ductal dilatation (⩾ 3 mm) was also evaluated on enhanced CT and MRI.

The degree of tumor attenuation relative to the surrounding pancreatic parenchyma during each CT phase was evaluated using a 4-point scale where grade 1 indicated low attenuation, grade 2 indicated iso-attenuation, grade 3 indicated mildly high attenuation, and grade 4 indicated high attenuation. Homogeneity (homogenous or heterogeneous) of tumor contrast enhancement during early phase enhanced CT was evaluated.

Table 1 Magnetic resonance imaging sequences and parameters

	TR (ms)	TE (ms)	FA (°)	Thickness (mm)	ETL	Matrix Size	FOV (mm)
Chemical-shift MRI							
2D dual GRE with 1.5-T system (n = 15)	128-133	2.2-2.4, 4.4-4.8	70-75	4-7	-	134-205 × 256	320-380
2D dual GRE with 3.0-T system (n = 4)	197-238	1.2, 2.4	60	5-5.5	-	192-200 × 192-200	350-360
3D dual GRE with 3.0-T system (n = 10)	5.8	1.2, 2.4	10	2.5	-	192 × 256	350
Fat-suppressed T2-weighted imaging							
Breath-hold half-Fourier single-shot TSE with 1.5-T system (n = 9)	Infinity	90	90	4-7	138	256 × 256	320-380
Respiratory-triggered multi-shot TSE with 1.5-T system (n = 6)	Respiratory intervals	80-85	90	5-6	15	256 × 336	320-350
Respiratory-triggered multi-shot TSE with 3.0-T system (n = 14)	Respiratory intervals	70-80	90	4-6	11-18	256-384 × 320-512	320-360

CT: Computed tomography; MRI: Magnetic resonance imaging; GRE: Gradient-echo; TSE: Turbo spin-echo; TR: Repetition time; TE: Echo time; FA: Flip angle; ETL: Echo train length; FOV: Field of view.

The readers were also asked to assess the following MRI characteristics: (1) predominant signal intensity on fat-suppressed T2-weighted images that was lower than, the same as, mildly higher, or higher than that of pancreatic parenchyma; (2) tumor homogeneity (homogenous or heterogeneous) on fat-suppressed T2-weighted MRI; (3) signal intensity of in-phase and out-of-phase images that was lower than, the same as, or higher than that of pancreatic parenchyma; and (4) the presence of intravoxel lipid, represented by high signal intensity on subtraction chemical shift MR images.

Any discrepancies were resolved during a third analysis session, in which a decision was reached by consulting with a third radiologist with 16 years of experience in abdominal radiology. The readers knew that the patients had PanNETs, but were blinded to the results of the histopathological analyses.

Quantitative MRI analysis

The signal intensities of in-phase and out-of-phase images were measured with an electronic cursor using oval or circular regions of interest (ROIs). To minimize bias on the measurements, a radiologist with 13 years of experience in abdominal radiology who did not attend the qualitative imaging analysis and had no knowledge of the histopathological or qualitative imaging findings, placed ROIs as large as possible within the PanNETs (mean size, 234 mm^2; range, 10-4194 mm^2). Cystic, hemorrhagic, and calcified components in the tumor were excluded from the ROIs whenever possible. The radiologist attempted to avoid causing a partial volume artifact at the edge of the tumor within the ROIs, and to place the ROIs in identical sites and sizes for in-phase and out-of-phase images in each patient.

The following quantitative parameter of signal changes between in-phase and out-of-phase images was calculated from the data acquired: signal intensity index which = [(tumor signal intensity on in-phase imaging - tumor signal intensity on out-of-phase imaging)/(tumor signal intensity on in-phase imaging)] × 100%.

Statistical analysis

We examined the CT and MRI features of ADRP-positive (lipid-rich) PanNETs to clarify the imaging characteristics in comparison with ADRP-negative (non-lipid-rich) PanNETs. Statistical analyses were performed using SPSS 14.0 software for Windows (SPSS version 14.0, Chicago, IL, United States). Fisher's exact test was used to compare patient gender, the presence of hormonal syndrome, tumor location, pathological tumor grade (G 1 *vs* G 2-3), the presence of clear cells, tumor margin, the presence of upstream main pancreatic duct dilatation, tumor homogeneity on the early phase enhanced CT and fat-suppressed T2-weighted imaging, and the presence of intravoxel lipid on the subtraction chemical shift MRI. Patient age, tumor size, TNM stage, visual grade of tumor attenuation on CT and signal intensity on T1- and T2-weighted images, and signal intensity index were compared between lipid-rich and non-lipid-rich PanNETs by Mann-Whitney U test. For all statistical analyses, a P value < 0.05 was considered statistically significant.

Kappa and weighted-kappa analyses were used to determine interobserver agreement for TNM stage, tumor margin, upstream main pancreatic duct dilatation, and visual tumor attenuation on CT and tumor signal intensity on T1-weighted, T2-weighted, and subtraction chemical-shift images, as well as tumor homogeneities on the early phase enhanced CT and T2-weighted MRI[23].

The statistical methods of this study were mainly reviewed by Yoshihiko Fukukura from Kagoshima University Graduate School of Medical and Dental Sciences.

RESULTS

Lipid-rich PanNETs were identified by ADRP-positive immunostaining in 12 of 29 patients (41.4%), and 15 of the 34 PanNETs (44.1%) contained some portion

Table 2 Comparison of clinical characteristics and TNM stage in 29 patients with lipid-rich or non-lipid-rich pancreatic neuroendocrine tumors

	Patients with lipid-rich PanNET (n = 12)	Patients with non-lipid-rich PanNET (n = 17)	P value
Age (yr)	52.6 ± 18.3	58.1 ± 15.0	0.478[1]
Sex			1.000[2]
Male	5	8	
Female	7	9	
Hormonal syndrome			1.000[2]
Functioning	6	8	
Non-functioning	6	9	
TNM stage			0.048[1]
Ⅰ	3	11	
Ⅱ	6	4	
Ⅲ	1	1	
Ⅳ	2	1	

[1]The P value levels shown were followed by the Mann-Whitney U test; [2]The P value levels shown were followed by Fisher's exact test. PanNET: Pancreatic neuroendocrine tumor.

(3% to 70%, mean 23.4%) of ADRP-positive lipid-rich cells.

There were no significant differences between patients with lipid-rich PanNETs and those with non-lipid-rich PanNETs in terms of age, gender, or the presence of hormonal syndrome (P = 0.478, 1.000, and 1.000, respectively) (Table 2). Fourteen patients were in Stage Ⅰ, 10 patients in Stage Ⅱ, two patients in Stage Ⅲ, and three patients in Stage Ⅳ (κ = 0.97). The TNM stage was higher in patients with lipid-rich PanNETs than that in those with non-lipid-rich PanNETs (P = 0.048).

Details including tumor size, location, pathological grade, and the presence of clear cells of all PanNETs are provided in Table 3. Lipid-rich PanNETs were significantly larger than non-lipid-rich PanNETs (28.8 ± 26.2 mm *vs* 20.5 ± 16.9 mm, P = 0.039). Tumor location (P = 0.184) was not significantly different between lipid-rich and non-lipid-rich PanNETs. On the basis of WHO classification, there were 22 G1 tumors, 11 G2 tumors, and one G3 tumor; there were no significant differences in pathological grade between lipid-rich and non-lipid-rich PanNETs (P = 0.288). Eight tumors (23.5%) in five patients (17.2%) contained clear cells at percentages ranging from 3% to 40%, mean 18.5%. Clear cells were found only in ADRP-positive lipid-rich PanNETs, and the association of clear cells with lipid-rich PanNETs was significant (8 of 15 ADRP-positive tumors, 53.3%, *vs* 0 of 19 ADRP-negative tumors, 0%, P < 0.001). All four PanNETs in a patient with von Hippel-Lindau disease contained ADRP-positive lipid-rich cells and clear cells. In two patients with MEN-1, two of four PanNETs contained ADRP-positive lipid-rich cells, but no clear cells were identified in any PanNETs. Nine of 26 patients (34.6%) who did not have any evidence of familial syndromes had lipid-rich PanNETs.

Table 3 Comparison of histopathological findings in lipid-rich *vs* non-lipid-rich pancreatic neuroendocrine tumors

	Lipid-rich PanNET (n = 15)	Non-lipid-rich PanNET (n = 19)	P value
Tumor size (mm)	28.8 ± 26.2	20.5 ± 16.9	0.039[1]
Location			0.679[2]
Head	7	7	
Body	5	5	
Tail	3	7	
Pathological grade			0.288[2]
Grade 1	8	14	
Grade 2-3	7	5	
Clear cells			< 0.001[2]
Present	8	0	
Absent	7	19	

[1]The P value levels shown were followed by the Mann-Whitney U test; [2]The P value levels shown were followed by Fisher's exact test. PanNET: Pancreatic neuroendocrine tumor.

Comparison of qualitative CT and MRI parameters in lipid-rich and non-lipid-rich PanNETs are presented in Table 4. There were no significant differences in tumor margins (P = 0.697) or the presence of upstream main pancreatic duct dilatation (P = 0.672) between lipid-rich and non-lipid-rich PanNETs. The degree of tumor attenuation relative to the surrounding pancreatic parenchyma during each phase was not significantly different between lipid-rich and non-lipid-rich PanNETs (unenhanced CT, P = 0.128; early phase, P = 0.888; portal venous phase, P = 0.443; delayed phase, P = 0.359). There was no significant difference in tumor homogeneity on early phase enhanced CT (P = 1.000) or fat-suppressed T2-weighted MRI (P = 0.484). No significant difference between tumor types was observed in terms of signal intensity on in-phase (P = 0.698), out-of-phase (P = 0.057), or fat-suppressed T2-weighted MR images (P = 0.798). Four of the 15 lipid-rich PanNETs exhibited high signal intensity on subtraction chemical shift MRI, and the association of high signal intensity on subtraction imaging with lipid-rich PanNETs was significant (4 of 15 lipid-rich PanNETs, 26.73%, *vs* 0 of 19 non-lipid-rich PanNETs, 0%, P = 0.029) (Figures 1 and 2). Interobserver agreement was substantial to almost perfect for the features described in the qualitative analysis.

In quantitative terms, the signal intensity index of lipid-rich PanNETs was significantly higher than that of the non-lipid-rich PanNETs (0.6% ± 14.1% *vs* -10.4% ± 14.4%, P = 0.004) (Figure 3). Eight of 15 lipid-rich PanNETs, *vs* 0 of 19 non-lipid-rich PanNETs, had positive signal intensity index values. All four of the tumors that were visually classified as high intensity on subtraction MRI also exhibited positive signal intensity index values.

DISCUSSION

The lipid-rich variant of PanNET contains clear cells

Table 4 Comparison of qualitative computed tomography and magnetic resonance imaging parameters in lipid-rich and non-lipid-rich pancreatic neuroendocrine tumors

Qualitative variables	Lipid-rich PanNET (n = 15)	Non-lipid-rich PanNET (n = 19)	P value	κ
Tumor margin			0.697[2]	0.92
Sharp	12	13		
Irregular	3	6		
Upstream pancreatic duct dilatation			0.672[2]	1.00
Present	4	3		
Absent	11	16		
Tumor attenuation on unenhanced CT			0.128[1]	0.99
Low	3	1		
Iso	12	17		
Mildly high	0	1		
High	0	0		
Tumor attenuation on early phase			0.888[1]	0.96
Low	0	2		
Iso	2	0		
Mildly high	4	5		
High	9	12		
Tumor attenuation on portal venous phase			0.443[1]	0.81
Low	0	1		
Iso	4	6		
Mildly high	6	7		
High	5	5		
Tumor attenuation on delayed phase			0.359[1]	0.75
Low	1	1		
Iso	6	12		
Mildly high	5	2		
High	3	4		
Tumor homogeneity on early phase			1.000[2]	0.77
Homogenous	8	11		
Heterogeneous	7	8		
Signal intensity on T2-weighted image			0.798[1]	0.98
Lower intensity	1	4		
Same intensity	3	2		
Mildly higher intensity	5	5		
Higher intensity	6	8		
Tumor homogeneity on T2-weighted image			0.484[2]	0.77
Homogenous	8	13		
Heterogeneous	7	6		
Signal intensity on in-phase image			0.698[1]	0.79
Lower intensity	14	17		
Same intensity	1	2		
Higher intensity	0	0		
Signal intensity on out-of-phase image			0.057[1]	0.89
Lower intensity	13	10		
Same intensity	1	8		
Higher intensity	1	1		
Intravoxel lipid on subtraction image			0.029[2]	1.00
Present	4	0		
Absent	11	19		

[1]The P value levels shown were followed by the Mann-Whitney U test; [2]The P value levels shown were followed by Fisher's exact test. PanNET: Pancreatic neuroendocrine tumor; CT: Computed tomography.

or cells with reticulated and vacuolated cytoplasm, depending on the amount of lipid, under light microscopy[3-7]. Because the vesicles forming the cytoplasm are clear, lipid-rich PanNETs have occasionally been classified as clear cell PanNETs[5]. However, very frequently cytoplasmic lipids are nearly indistinguishable from glycogen or mucin inclusions in the cytoplasm because both appear as unstained vesicles upon hematoxylin-eosin staining. ADRP is a lipid droplet-associated protein that coats cytoplasmic lipid droplets, and is a specific marker for diseases characterized by lipid accumulation[24,25]. We therefore performed immunohistochemical ADRP staining to check for lipid-rich cells in PanNETs. ADRP-positive lipid-rich cells were observed in 15 of 34 tumors (44.1%), and clear cells were observed in 8 (23.5%). The results can be explained by the fact that ADRP immunohistochemistry offers a more sensitive technique to demonstrate lipid droplets compared with hematoxylin-eosin staining[24]. Physicians should be aware that there is a considerable amount of cytoplasmic lipid in PanNETs.

Lipid-rich PanNETs are strongly associated with von Hippel-Lindau disease[4] and MEN-1[6]. It is reported that 60% of von Hippel-Lindau disease-associated PanNETs will exhibit at least focal clear-cell cytology[4]. In our study, all four PanNETs in a patient with von Hippel-Lindau disease contained ADRP-positive lipid-rich cells and clear cells. Fryer *et al*[6] reported that PanNETs contained lipid-rich cells either focally or entirely in six of 16 patients (37.5%) with MEN-1. In our two patients with MEN-1, two of four PanNETs contained ADRP-positive lipid-rich cells. The frequency of lipid-rich PanNETs in patients without MEN-1 or von Hippel-Lindau disease has been obscure. Nine of 26 patients (34.6%) in our series who did not have any evidence of familial syndromes had ADRP-positive lipid-rich PanNETs. Therefore, the lipid-rich variant of PanNETs may be not as rare as previously reported[3,5], although further study is needed to clarify the prevalence of lipid-rich or clear cell variants of PanNETs in a larger study population.

Singh *et al*[5] reported that lipid-rich PanNETs tended to be larger than conventional PanNETs, have histologically more diffuse growth patterns, and have a vascular pattern that has a more sinusoidal quality. Enhanced CT and MRI are useful not only for detecting and staging PanNETs, but also for tumor characterization[8,9]. In our study, there were no significant differences in the appearances of the tumor margins between lipid-rich and non-lipid-rich PanNETs. However, lipid-rich PanNETs were significantly larger than non-lipid-rich PanNETs (P = 0.039), and TNM stage was higher in patients with lipid-rich PanNETs than that in those with non-lipid-rich PanNETs (P = 0.048).

It is important to clarify CT and MRI findings of lipid-rich PanNETs and differentiate them from other pancreatic lesions, as its substantial deviation from the usual histopathological appearance often poses a diagnostic problem in biopsy[3-7]. We examined CT and MRI features of lipid-rich PanNETs in comparison with non-lipid-rich PanNETs. The degree and homogeneity of tumor attenuation on qualitative CT analysis were not significantly different between lipid-rich and non-lipid-rich PanNETs, and there was no significant difference in the degree or homogeneity of signal intensity on T1- and T2-weighted images between lipid-rich and

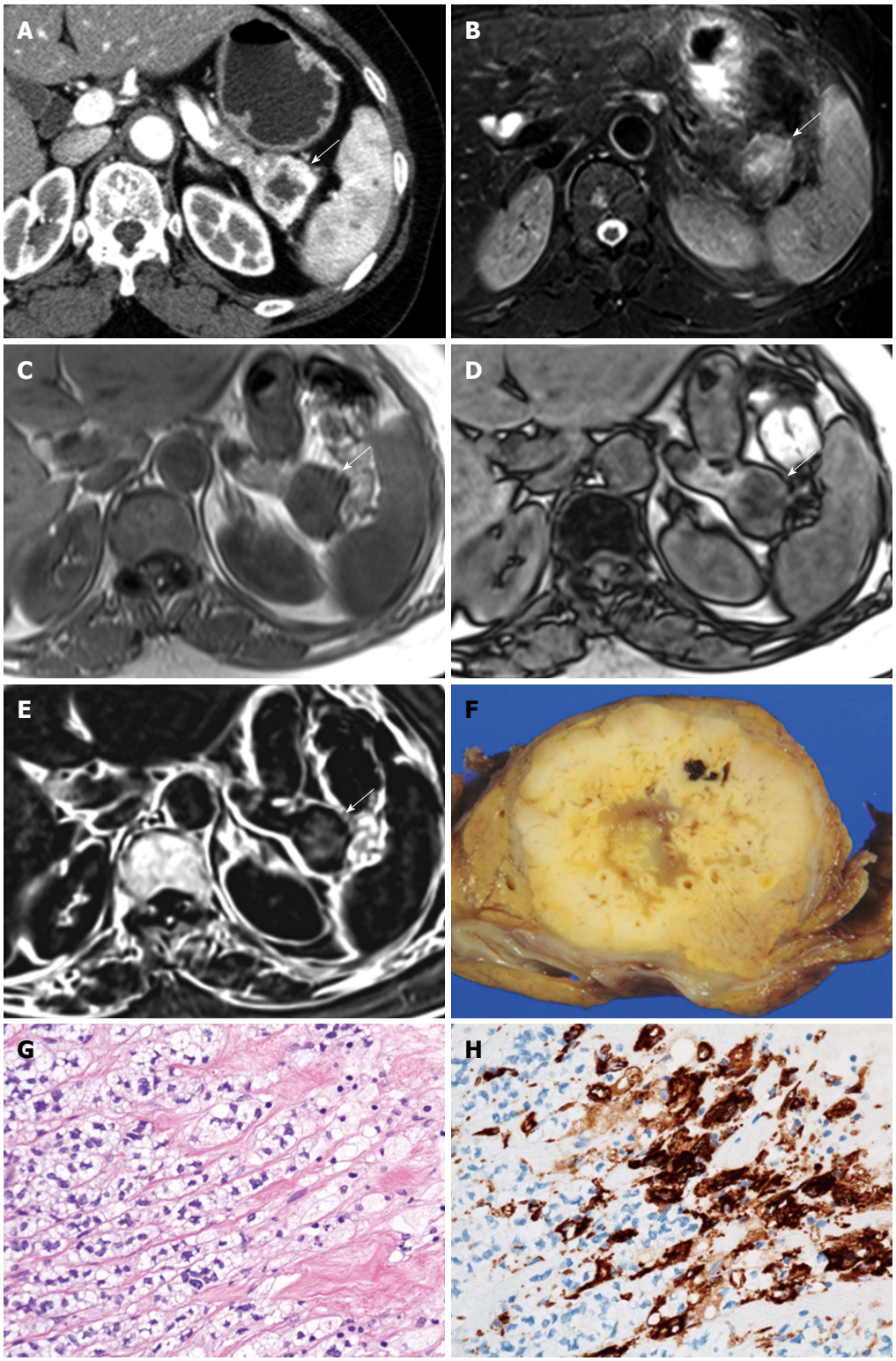

Figure 1 Lipid-rich pancreatic neuroendocrine tumor in a 64-year-old woman. A: Axial early phase enhanced computed tomography shows a 30 mm well-circumscribed tumor (arrow) with thick and marked contrast enhancement only at the periphery; B: The tumor shows heterogeneous high signal intensity (arrow) on fat-suppressed T2-weighted images (4200/71); C and D: In-phase (5.8/2.4, 10°) (C) and out-of-phase (5.8/1.2, 10°) images with 3D technique (D) show a substantial drop in tumor signal intensity (arrow) from the in-phase (209.6) to the out-of-phase (137.5) image, resulting in a signal intensity index of 34.4%; E: The subtraction image shows apparent high signal intensity (arrow), indicating the presence of lipid component; F: Grossly, the pancreatic NET is a well-circumscribed yellowish color lesion; G: Microscopically, the tumor cells have abundant microvesicular cytoplasm; H: Adipose differentiation-related protein (ADRP) is expressed in the cytoplasm of tumor cells. The staining area is a microvesicular pattern as droplets.

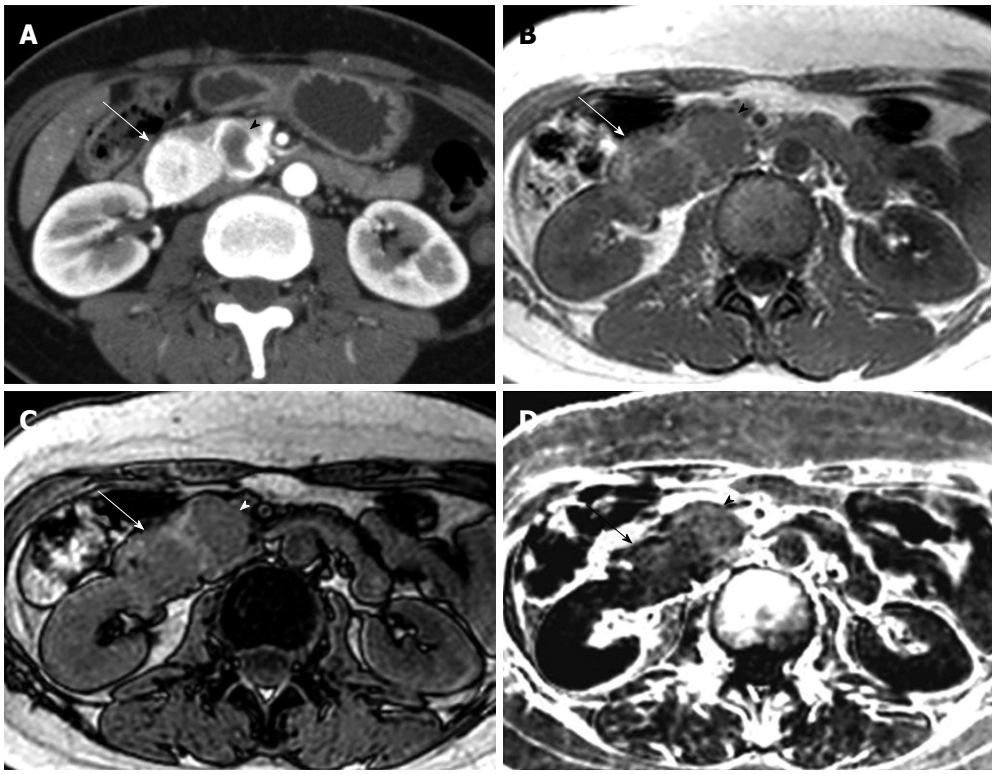

Figure 2 Lipid-rich pancreatic neuroendocrine tumors in a 49-year-old woman with von-Hippel-Lindau disease. A: Axial early phase enhanced computed tomography shows a 30 mm tumor with homogenous enhancement (arrow) and a 24 mm tumor with marked peripheral enhancement (arrow head) in the head of the pancreas; B and C: In-phase (134/2.4, 60°) (B) and out-of-phase (134/1.2, 60°) images with 2D technique (C) show a substantial drop in tumor signal intensity from the in-phase [813.0 (arrow) and 819.5 (arrow head)] to the out-of-phase [783.2 (arrow) and 775.3 (arrow head)] image, resulting in signal intensity indexes of 3.7% (arrow) and 5.4% (arrow head), respectively; D: The subtraction image shows apparent high signal intensity (arrow and arrow head).

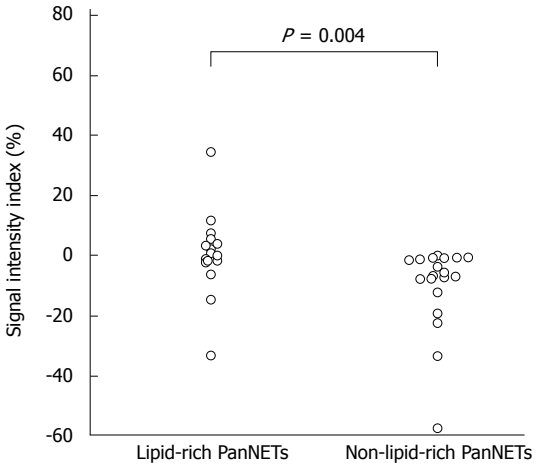

Figure 3 Scatterplot showing the differences in signal intensity index between lipid-rich and non-lipid-rich pancreatic neuroendocrine tumors. Eight of 15 lipid-rich pancreatic neuroendocrine tumors (PanNETs) exhibit positive signal intensity index values, whereas 0 of 19 non-lipid-rich PanNETs show positive values. The signal intensity index is significantly higher in lipid-rich than in non-lipid-rich PanNETs (P = 0.004).

non-lipid-rich PanNETs. Thus, our results indicate that lipid-rich PanNETs have a similar appearance to usual PanNETs on enhanced CT and conventional MRI.

It has been suggested that chemical shift MRI is more sensitive and specific for detecting lipids than other radiologic modalities, including ultrasonography, CT, and conventional MRI[11]. The signal on out-of-phase images is expected to be almost equal to or slightly higher than that of in-phase images when the ROI contained no lipids[26,27]. When a lipid component is present, the signal on the out-of-phase images should be smaller than that of the in-phase images, and the signal intensity index shows positive. In our study, there were significant differences in the signal intensity index between lipid-rich and non-lipid-rich PanNETs (P = 0.004). Eight PanNETs (23.5%) had positive signal intensity index values, and all of them also contained ADRP-positive lipid-rich cells at pathology, while 0 of 19 ADRP-negative PanNETs displayed positive values. Four of the eight PanNETs that exhibited a positive signal intensity index were classified as high intensity tumors on the subtraction images during qualitative analysis, which was consistent with lipid content. Thus, these results suggest that chemical shift MRI is sensitive and specific enough to demonstrate cytoplasmic lipids in lipid-rich PanNETs. Moreover, PanNETs in which lipid components are visualized on chemical shift MRI may be not rare.

Several pancreatic lesions, including focal fatty replacement[13-15], lipoma[14], liposarcoma[14], teratoma[14], lymphoepithelial cyst[16], and pancreatic metastases from clear cell renal cell carcinoma[17] and hepatocellular carcinoma[18] have been reported to have lipid components that are visualized on ultrasonography,

CT, or MRI. To the best of our knowledge, this is the first report of PanNETs in which lipid components are visualized on chemical shift MRI. Among tumors in which lipid components can be visualized on ultrasonography, CT, or MRI, metastases from clear cell renal cell carcinoma[28] or hepatocellular carcinoma[29,30] are usually hyperattenuated during the early or portal venous phases of contrast-enhanced CT and MRI. Therefore, it might be difficult to differentiate between lipid-rich PanNETs and metastatic renal cell carcinoma or hepatocellular carcinoma, because all of these tumors have similar contrast enhancement patterns and signal intensities on MRI. In cases of suspected metastatic renal cell or hepatocellular carcinoma, the value of clinical history is emphasized, and in cases of functioning PanNETs, elevated hormone levels and symptoms related to high hormone levels should also assist with the differential diagnosis.

Some limitations in our study must be considered. First, this study included a relatively small number of patients. A larger study would be required to definitively establish the characteristic features of lipid-rich PanNETs. Second, the series included only one WHO grade 3 PanNET, and thus may not represent the entire spectrum of lipid-rich PanNETs. WHO grade 3 PanNETs are not usually targeted for surgical resection, and biopsy specimens cannot be used for evaluating the correct presence of cytoplasmic lipids in the tumor.

In conclusion, ADRP-positive lipid-rich cells were observed in 15 of 34 PanNETs (44.1%), and clear cells were observed in 8 (23.5%). Lipid-rich PanNETs had a similar appearance to usual PanNETs on enhanced CT and conventional MRI. On chemical shift MRI, however, positive signal intensity index values in concordance with lipid contents were observed in eight (23.5%) of 34 PanNETs and in four PanNETs (11.8%) the presence of cytoplasmic lipids in the tumors was visually suspected. The lipid-rich variant of PanNET should be included in the differential diagnosis whenever chemical shift MRI demonstrates lipid components within hypervascular pancreatic tumors.

COMMENTS

Background

Lipid-rich tumor is a distinct histological variant of pancreatic neuroendocrine tumor (PanNET) that has cells characterized by an abundant, clear, and vacuolated cytoplasm, which can pose diagnostic problems at biopsy because of a substantial deviation from the usual appearance.

Research frontiers

Radiologic detection of lipid components within pancreatic lesions has been evaluated for a variety of pancreatic lesions. However, computed tomography (CT) and magnetic resonance imaging (MRI) features of lipid-rich PanNETs have not yet been described. Moreover, there have been no reports regarding the utility of chemical shift MRI for the detection of intracytoplasmic lipids associated with lipid-rich PanNETs. Knowledge of CT and MRI findings of lipid-rich PanNETs is important for arriving at the correct diagnosis of PanNET. This study was designed to clarify CT and MRI findings of lipid-rich PanNETs.

Innovations and breakthroughs

Lipid-rich PanNETs have a similar appearance to usual PanNETs on enhanced CT and conventional MRI. On chemical shift MRI, positive signal intensity index values in concordance with lipid contents were observed in eight of 34 PanNETs (23.5%).

Applications

Lipid-rich PanNETs should be included in differential diagnosis whenever chemical shift MRI demonstrates lipid components within hypervascular pancreatic tumors.

Terminology

Chemical shift MRI has been clinically applied in the field of body imaging to detect small amounts of lipids based on the inherent difference in the resonant frequencies of water and fat protons.

Peer-review

The authors clarify the CT and MRI characteristics of lipid-rich PanNETs, which is of clinical importance.

REFERENCES

1 **Ramage JK**, Ahmed A, Ardill J, Bax N, Breen DJ, Caplin ME, Corrie P, Davar J, Davies AH, Lewington V, Meyer T, Newell-Price J, Poston G, Reed N, Rockall A, Steward W, Thakker RV, Toubanakis C, Valle J, Verbeke C, Grossman AB. Guidelines for the management of gastroenteropancreatic neuroendocrine (including carcinoid) tumours (NETs). *Gut* 2012; **61**: 6-32 [PMID: 22052063 DOI: 10.1136/gutjnl-2011-300831]

2 **Halfdanarson TR**, Rabe KG, Rubin J, Petersen GM. Pancreatic neuroendocrine tumors (PNETs): incidence, prognosis and recent trend toward improved survival. *Ann Oncol* 2008; **19**: 1727-1733 [PMID: 18515795 DOI: 10.1093/annonc/mdn351]

3 **Capelli P**, Martignoni G, Pedica F, Falconi M, Antonello D, Malpeli G, Scarpa A. Endocrine neoplasms of the pancreas: pathologic and genetic features. *Arch Pathol Lab Med* 2009; **133**: 350-364 [PMID: 19260741 DOI: 10.1043/1543-2165-133.3.350]

4 **Lubensky IA**, Pack S, Ault D, Vortmeyer AO, Libutti SK, Choyke PL, Walther MM, Linehan WM, Zhuang Z. Multiple neuroendocrine tumors of the pancreas in von Hippel-Lindau disease patients: histopathological and molecular genetic analysis. *Am J Pathol* 1998; **153**: 223-231 [PMID: 9665483]

5 **Singh R**, Basturk O, Klimstra DS, Zamboni G, Chetty R, Hussain S, La Rosa S, Yilmaz A, Capelli P, Capella C, Cheng JD, Adsay NV. Lipid-rich variant of pancreatic endocrine neoplasms. *Am J Surg Pathol* 2006; **30**: 194-200 [PMID: 16434893]

6 **Fryer E**, Serra S, Chetty R. Lipid-rich ("clear cell") neuroendocrine tumors of the pancreas in MEN I patients. *Endocr Pathol* 2012; **23**: 243-246 [PMID: 22923265 DOI: 10.1007/s12022-012-9221-z]

7 **Ordóñez NG**, Silva EG. Islet cell tumour with vacuolated lipid-rich cytoplasm: a new histological variant of islet cell tumour. *Histopathology* 1997; **31**: 157-160 [PMID: 9279567]

8 **Horton KM**, Hruban RH, Yeo C, Fishman EK. Multi-detector row CT of pancreatic islet cell tumors. *Radiographics* 2006; **26**: 453-464 [PMID: 16549609]

9 **Lewis RB**, Lattin GE, Paal E. Pancreatic endocrine tumors: radiologic-clinicopathologic correlation. *Radiographics* 2010; **30**: 1445-1464 [PMID: 21071369 DOI: 10.1148/rg.306105523]

10 **Manfredi R**, Bonatti M, Mantovani W, Graziani R, Segala D, Capelli P, Butturini G, Mucelli RP. Non-hyperfunctioning neuroendocrine tumours of the pancreas: MR imaging appearance and correlation with their biological behaviour. *Eur Radiol* 2013; **23**: 3029-3039 [PMID: 23793519 DOI: 10.1007/s00330-013-2929-4]

11 **Dixon WT**. Simple proton spectroscopic imaging. *Radiology* 1984; **153**: 189-194 [PMID: 6089263]

12 **Fujiyoshi F**, Nakajo M, Fukukura Y, Tsuchimochi S. Characterization of adrenal tumors by chemical shift fast low-angle

shot MR imaging: comparison of four methods of quantitative evaluation. *AJR Am J Roentgenol* 2003; **180**: 1649-1657 [PMID: 12760936]
13 **Matsumoto S**, Mori H, Miyake H, Takaki H, Maeda T, Yamada Y, Oga M. Uneven fatty replacement of the pancreas: evaluation with CT. *Radiology* 1995; **194**: 453-458 [PMID: 7824726]
14 **Katz DS**, Hines J, Math KR, Nardi PM, Mindelzun RE, Lane MJ. Using CT to reveal fat-containing abnormalities of the pancreas. *AJR Am J Roentgenol* 1999; **172**: 393-396 [PMID: 9930790]
15 **Kim HJ**, Byun JH, Park SH, Shin YM, Kim PN, Ha HK, Lee MG. Focal fatty replacement of the pancreas: usefulness of chemical shift MRI. *AJR Am J Roentgenol* 2007; **188**: 429-432 [PMID: 17242252]
16 **Fukukura Y**, Inoue H, Miyazono N, Kajiya Y, Fujiyoshi F, Yano T, Sakoda K, Tanaka S, Aiko T, Nakajo M. Lymphoepithelial cysts of the pancreas: demonstration of lipid component using CT and MRI. *J Comput Assist Tomogr* 1998; **22**: 311-313 [PMID: 9530401]
17 **Carucci LR**, Siegelman ES, Feldman MD. Pancreatic metastasis from clear cell renal carcinoma: diagnosis with chemical shift MRI. *J Comput Assist Tomogr* 1999; **23**: 934-936 [PMID: 10589569]
18 **Nishiofuku H**, Marugami N, Tanaka T, Anai H, Maeda S, Masada T, Takano M, Mitoro A, Kichikawa K. Isolated fat-containing pancreatic metastasis from hepatocellular carcinoma. *Jpn J Radiol* 2013; **31**: 408-411 [PMID: 23539254 DOI: 10.1007/s11604-013-0193-9]
19 **Klimstra DS**, Arnold R, Capella C, Hrunan RH, Klöppel G. Neuroendocrine neoplasms of the pancreas. In: Bosman FT, Carneiro F, Hruban RH, Theise ND, editors. WHO classification of tumours of the digestive system. Lyon: IARC, 2010: 322-326
20 **Rindi G**, Klöppel G, Alhman H, Caplin M, Couvelard A, de Herder WW, Erikssson B, Falchetti A, Falconi M, Komminoth P, Körner M, Lopes JM, McNicol AM, Nilsson O, Perren A, Scarpa A, Scoazec JY, Wiedenmann B. TNM staging of foregut (neuro)endocrine tumors: a consensus proposal including a grading system. *Virchows Arch* 2006; **449**: 395-401 [PMID: 16967267]
21 **Lu DS**, Reber HA, Krasny RM, Kadell BM, Sayre J. Local staging of pancreatic cancer: criteria for unresectability of major vessels as revealed by pancreatic-phase, thin-section helical CT. *AJR Am J Roentgenol* 1997; **168**: 1439-1443 [PMID: 9168704]
22 **Roche CJ**, Hughes ML, Garvey CJ, Campbell F, White DA, Jones L, Neoptolemos JP. CT and pathologic assessment of prospective nodal staging in patients with ductal adenocarcinoma of the head of the pancreas. *AJR Am J Roentgenol* 2003; **180**: 475-480 [PMID: 12540455]
23 **Landis JR**, Koch GG. An application of hierarchical kappa-type statistics in the assessment of majority agreement among multiple observers. *Biometrics* 1977; **33**: 363-374 [PMID: 884196]
24 **Mak KM**, Ren C, Ponomarenko A, Cao Q, Lieber CS. Adipose differentiation-related protein is a reliable lipid droplet marker in alcoholic fatty liver of rats. *Alcohol Clin Exp Res* 2008; **32**: 683-689 [PMID: 18341646 DOI: 10.1111/j.1530-0277.2008.00624.x]
25 **Imai Y**, Varela GM, Jackson MB, Graham MJ, Crooke RM, Ahima RS. Reduction of hepatosteatosis and lipid levels by an adipose differentiation-related protein antisense oligonucleotide. *Gastroenterology* 2007; **132**: 1947-1954 [PMID: 17484887]
26 **Schindera ST**, Soher BJ, Delong DM, Dale BM, Merkle EM. Effect of echo time pair selection on quantitative analysis for adrenal tumor characterization with in-phase and opposed-phase MR imaging: initial experience. *Radiology* 2008; **248**: 140-147 [PMID: 18566172 DOI: 10.1148/radiol.2481071069]
27 **Marin D**, Soher BJ, Dale BM, Boll DT, Youngblood RS, Merkle EM. Characterization of adrenal lesions: comparison of 2D and 3D dual gradient-echo MR imaging at 3 T--preliminary results. *Radiology* 2010; **254**: 179-187 [PMID: 20032151 DOI: 10.1148/radiol.09090486]
28 **Ng CS**, Loyer EM, Iyer RB, David CL, DuBrow RA, Charnsangavej C. Metastases to the pancreas from renal cell carcinoma: findings on three-phase contrast-enhanced helical CT. *AJR Am J Roentgenol* 1999; **172**: 1555-1559 [PMID: 10350288]
29 **Choi BI**, Han JK, Cho JM, Choi DS, Han MC, Lee HS, Kim CY. Characterization of focal hepatic tumors. Value of two-phase scanning with spiral computed tomography. *Cancer* 1995; **76**: 2434-2442 [PMID: 8625068]
30 **Luca A**, Caruso S, Milazzo M, Mamone G, Marrone G, Miraglia R, Maruzzelli L, Carollo V, Minervini MI, Vizzini G, Gruttadauria S, Gridelli B. Multidetector-row computed tomography (MDCT) for the diagnosis of hepatocellular carcinoma in cirrhotic candidates for liver transplantation: prevalence of radiological vascular patterns and histological correlation with liver explants. *Eur Radiol* 2010; **20**: 898-907 [PMID: 19802612 DOI: 10.1007/s00330-009-1622-0]

P- Reviewer: Shen J, Storto G **S- Editor**: Yu J
L- Editor: Rutherford A **E- Editor**: Ma S

Published by **Baishideng Publishing Group Inc**
8226 Regency Drive, Pleasanton, CA 94588, USA
Telephone: +1-925-223-8242
Fax: +1-925-223-8243
E-mail: bpgoffice@wjgnet.com
Help Desk: http://www.wjgnet.com/esps/helpdesk.aspx
http://www.wjgnet.com

ISSN 1007-9327